



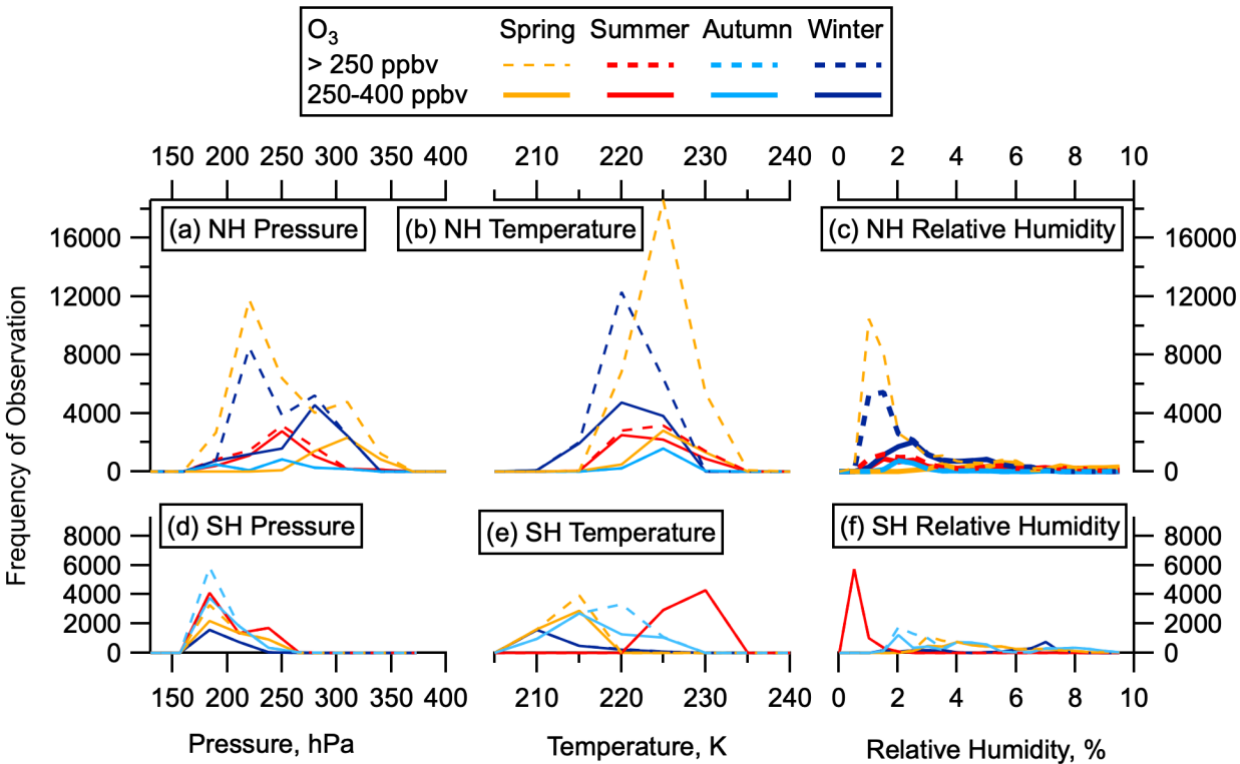
Supplement of

Large hemispheric difference in nucleation mode aerosol concentrations in the lowermost stratosphere at mid- and high latitudes

Christina J. Williamson et al.

Correspondence to: Christina J. Williamson (christina.williamson@noaa.gov)

The copyright of individual parts of the supplement might differ from the article licence.



20 **Figure S1: LMS thermodynamic conditions.** Histograms of Pressure (a, d), Temperature (b, e) and Relative Humidity (c, f) of observations in the NH and SH LMS respectively (ozone restricted to below 400 ppbv in solid lines).

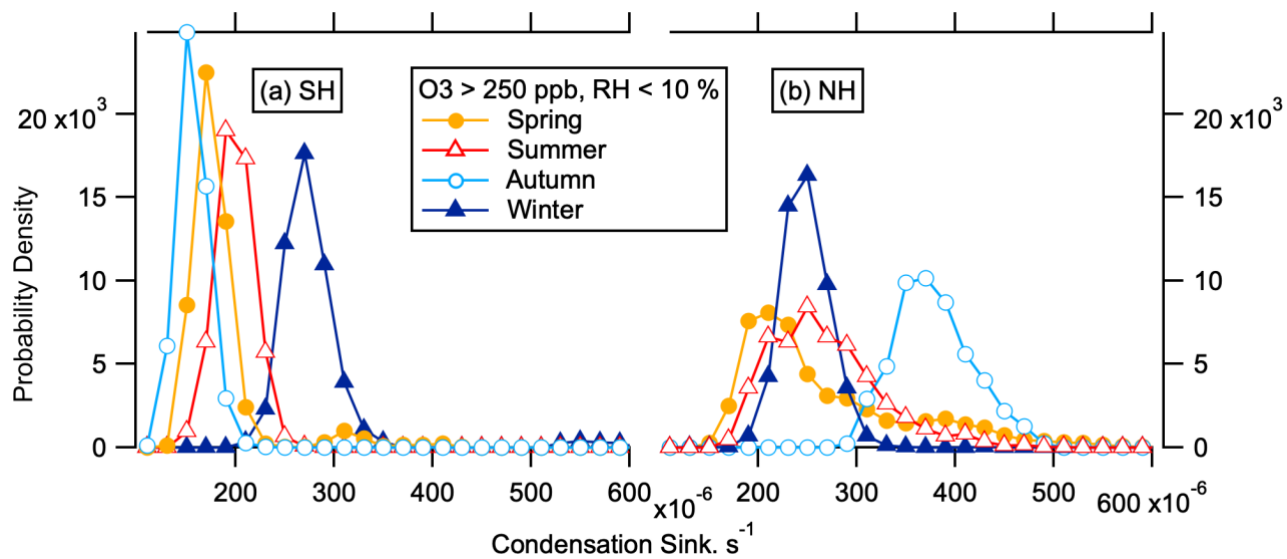


Figure S2: Condensation Sinks in the LMS. Histograms of condensation sinks calculated from size distributions measured in the LMS on ATom in the southern hemisphere (a) and northern hemisphere (b), separated by season.

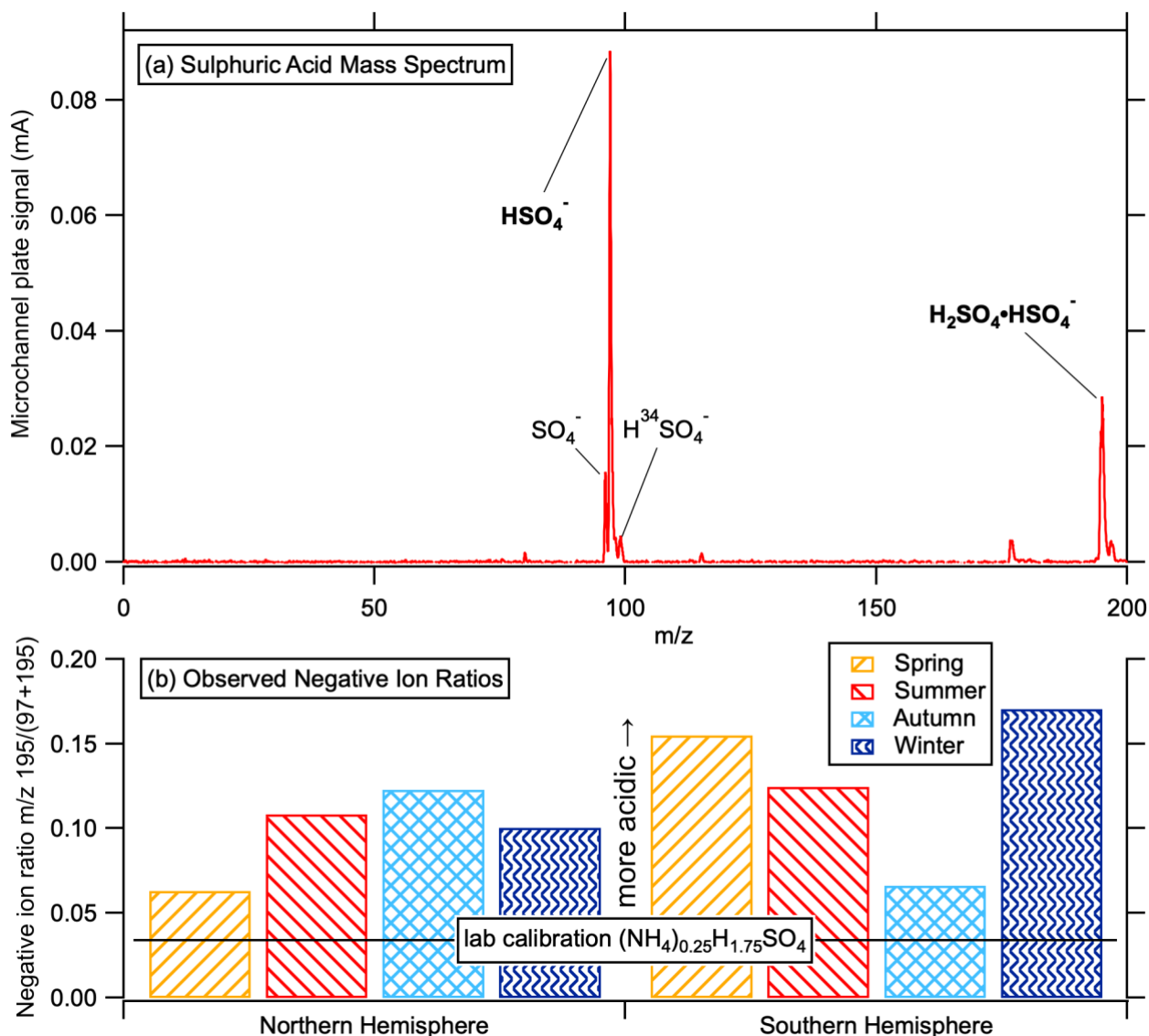


Figure S3: Aerosol acidity in the LMS. a) An example negative ion spectrum of an acidic sulphate particle. This spectrum is from a $0.39 \mu\text{m}$ diameter particle in the stratosphere at 12.2 km and 310 ppbv of O_3 on 20171009. Laboratory calibrations show that the $\text{H}_2\text{SO}_4 \cdot \text{HSO}_4^-$ peak is very small or non-existent for particles composed of ammonium sulphate and the cluster ion peak increases with acidity until it is a large peak for nearly pure sulfuric acid. b) The bars for the NH (left) and SH (right), separated by season, show the average ratio of the size of the cluster peak at m/z 195 to the sum of the peaks at m/z 195 and 97. The averages are for particles when O_3 concentrations were 250 to 350 ppbv in the stratosphere. The averages are also for particles between 0.35 and $0.6 \mu\text{m}$ diameter because in the stratosphere most particles of that size originated in the stratosphere. Lab calibrations of particles composed of $(\text{NH}_4)_{0.25}\text{H}_{1.75}\text{SO}_4$ had a negative ion ration m/z 195/(97+195) of 0.034, therefore we

35 consider ratios higher than this (more acidic) to contain less than 0.25 mole fraction ammonium. Rather than analyzing possible differences in the acidity with season, here we emphasize that stratospheric particles in all seasons and both hemispheres are highly acidic. This sets limits on the possible concentration of gas phase ammonia. Calculations of uptake from the gas phase show that a continuous 1 pptv of gas phase ammonia could add 0.25 mol fraction ammonium to sulfuric acid particles in less than a week.

40 **S2 Particle and SO₂ lifetimes in the LMS**

To interpret the small particles and SO₂ enhancements in the NH LMS, it is important to understand both their lifetimes, and also their residence times in the LMS. In winter and spring, seasonal flushing of the LMS limits residence time close to the tropopause to a few weeks. In summer and fall LMS circulation is governed by the monsoons, capping residence times at a few months (Yang et al., 2016; Orbe et al., 2014). The major influence on SO₂ lifetimes in the LMS is reaction with OH. SO₂ lifetime due to reaction with OH in the LMS has been estimated at about 1 month (Höpfner et al., 2015).

For particles, coagulation and growth via condensation are important factors in determining lifetimes at smaller sizes, and sedimentation into the troposphere becomes important at larger sizes. We have calculated coagulation lifetimes of nucleation mode particles with particles large enough that the resulting particle after coagulation is larger than 12 nm (Fig. S4). In the NH LMS these lifetimes range from 9 hours to 3 days in August, February and May, and up to 2.5 weeks in October. In the SH, due to much lower particle concentration, these lifetimes are on the order of weeks to months.

Growth with respect to sulphuric acid condensation was calculated following the method of Nieminen et al. (2010), giving

$$GR = \frac{C_{SA} \times 2M_{SA} \times cond_K}{\rho \pi d_p^2} \quad [1]$$

55 Where C_{SA} is the ambient concentration of sulphuric acid, M_{SA} is the mass of a sulphuric acid molecule, ρ is the density of sulphuric acid in liquid phase (assumed for both the condensing vapour and the particle), and $cond_K$ is in the rate coefficient (cm³/s) for the condensation of a sulphuric acid molecule on a particle of diameter d_p . This is calculated based on the Fuchs expression for the coagulation rate coefficient following Seinfeld and Pandis (2006).

60 For 10⁵-10⁷ cm⁻³ sulphuric acid, we calculate growth rates for nucleation mode particles in the NH LMS conditions ranging from 0.002 nm/h at the 10⁵ cm⁻³ sulphuric acid concentrations, 0.024 nm/h at the 10⁶ cm⁻³ sulphuric acid concentrations, and 0.3 nm/h at the 10⁷ cm⁻³ sulphuric acid concentrations for nucleation mode particles (Fig. S5). While this seems low for growth following a nucleation event compared to common literature values, we note that most prior calculations have been made for boundary layer conditions, and the lower temperatures in the LMS make slower growth rates plausible. Assuming a particle nucleates at around 2 nm, and elevated sulphuric acid concentrations present for 12 hours per day since it is photolytically

produced, it would grow out of the nucleation mode through condensation of sulphuric acid only within 1 year, 5 weeks or 3 days, depending on the amount of sulphuric acid. If sulphuric acid levels are low enough to lead to the 1-year or 5-week lifetimes, then coagulation or condensation including HOMs would control the nucleation mode lifetime, and growth from sulphuric acid condensation would not be an important factor.

70

Highly oxygenated organic molecules (HOMs) contribute to particle growth and formation in a variety of atmospheric environments (Bianchi et al., 2016; Bianchi et al., 2019; Andreae et al., 2018; Tröstl et al., 2016; Zhu et al., 2019). Concentrations of highly oxygenated molecules in the NH LMS as seen on ATom have been estimated to be on the order of pptv (Murphy et al., 2020), and box modelling shows maximum LMS sulfuric acid concentrations from 20 ppb SO₂ of up to around $2 \times 10^6 \text{ cm}^{-3}$ (Fig. 11). At 300 hPa and 230 K, 1 pptv is equivalent to $10^7 \text{ molecules cm}^{-3}$. Chamber experiments conducted at 248 K at around 1013 hPa with organics but no sulfuric acid, show growth rates from HOM concentrations of 10^7 cm^{-3} of around 1 nm h^{-1} (Stolzenburg et al., 2018). Chamber experiments conducted at sea-level conditions have calculated particle growth rates from concentrations of $10^7 \text{ molecules cm}^{-3}$ HOMs and sulfuric acid concentration between 10^4 and 10^6 cm^{-3} to be between 0.2 and 20 nm h^{-1} for 1.1 - 3.2 nm particles, and between 1 and 10 nm h^{-1} for particles larger than 5 nm (Tröstl et al., 2016). Observed growth rates from the Jungfraujoch High Alpine research station in February (ambient temperatures around 260 K) attributed to $2 \times 10^6 \text{ cm}^{-3}$ sulfuric acid were around 0.2 nm h^{-1} , and attributed to around $2 \times 10^6 \text{ cm}^{-3}$ HOMs were around 0.5 nm h^{-1} (Bianchi et al., 2016), giving a total for HOMs and SA similar to concentrations observed in the LMS of about 0.7 nm h^{-1} , though the temperature on JFJ was around 30 K warmer. If growth is close to the kinetic limit, we do not expect growth rates to vary with pressure, though temperature is likely a factor. While we are not aware of any examples of measured growth rates matching the all of the chemical, temperature and pressure conditions observed in the LMS for nucleation mode aerosol, the above examples indicate that growth rates between 0.2 and 10 nm h^{-1} are reasonable estimates for the NH LMS in the presence of HOMs. Assuming these growth rates are sustained for 12 hours per day (photochemical production of HOMs), this would lead to lifetimes between 1 hour and 4 days.

90 Growth from sulphuric acid, HOMs and coagulation all interact to determine the lifetime of nucleation mode aerosol in the LMS. Within the large uncertainties of the different processes indicated above, we can conclude that nucleation mode aerosol in the NH LMS have lifetimes on the order of hours to days.

Schroder et al. (2000) showed that despite the higher sinks in aircraft exhaust plume, the effective nucleation mode particle lifetime within the is ~ 1 - 2 days because particles are both emitted directly from the engines and form from the gas phase within concentrated and often supersaturated conditions of the plume. Lifetimes of nucleation mode aerosol in the SH LMS are longer than in the NH LMS, since both coagulation sinks and rate of growth out of the nucleation mode are lower due to lower particle and condensable vapour concentrations. However, lifetimes within aircraft plumes will be similar regardless of which hemisphere they are being emitted into, since they are dominated by the production and loss rates in the plume. Therefore, we

100 will assume a 2-day lifetime for nucleation mode particles in the LMS in both hemispheres, and not that this may lead to an underestimate of concentrations in the SH.

Sulphuric acid is produced in the LMS by oxidation of SO₂. This occurs in the presence of sunlight, with peak sulphuric acid concentrations occurring near the middle of the day (see Fig. 7). This causes nucleation involving sulphuric acid to occur with a diurnal cycle. No correlation is observed between nucleation mode number concentration and solar zenith angle (Fig. S6) in the NH LMS. This therefore puts a lower limit on the lifetime of nucleation mode aerosol in the NH LMS close to 12 hours.

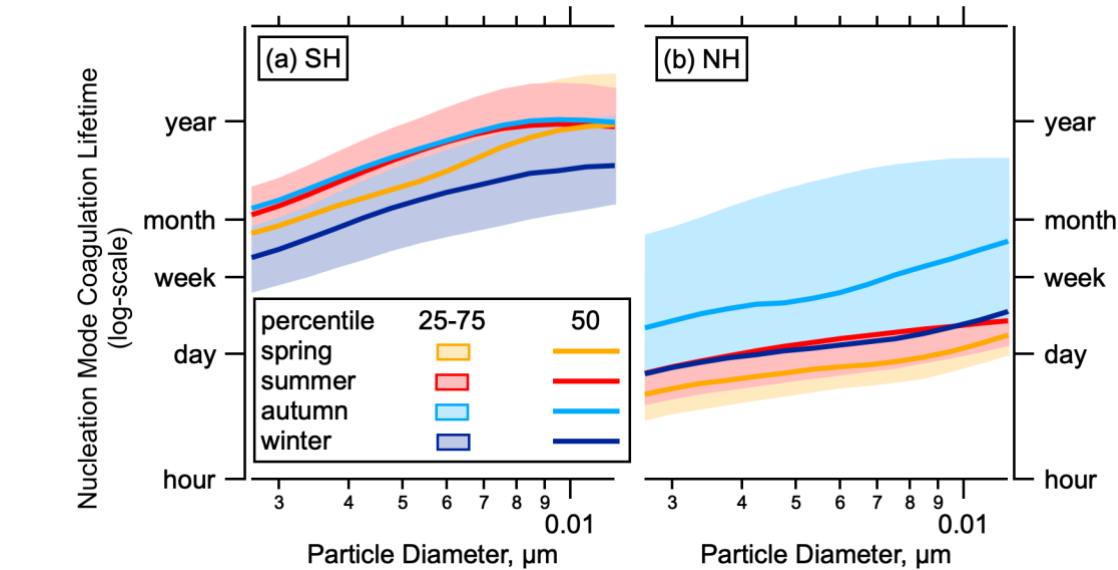


Figure S4: LMS nucleation mode lifetime with respect to coagulation. Calculated median and interquartile range of lifetimes of particles smaller than 12 nm with respect to coagulation that forms particles larger than 12 nm in the LMS (O₃ between 250 and 400 ppbv, RH <10 %) in the SH (a) and NH (b) for each season.

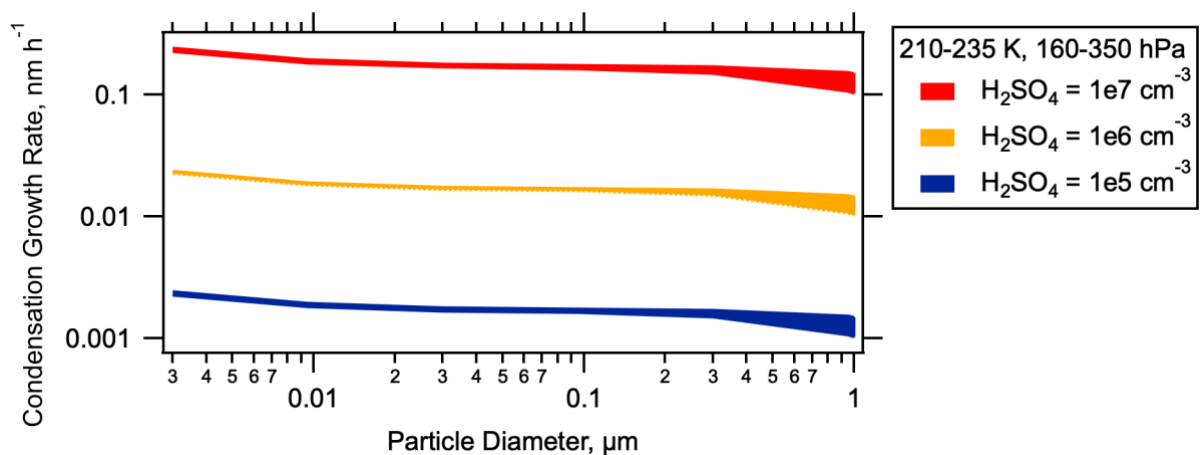


Figure S5: Condensation Growth Rates in the NH LMS. Condensation growth rates as a function of particle diameter, calculated for sulphuric acid (H_2SO_4) concentrations of 10^5 , 10^6 and 10^7 cm^{-3} (colours) under NH LMS conditions.

115

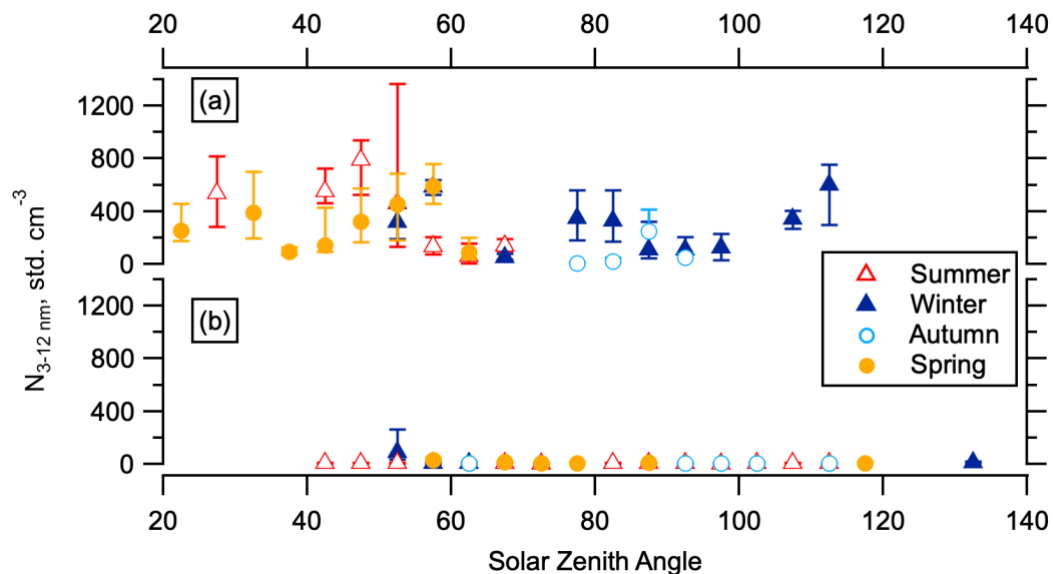


Figure S6: Relationship between nucleation mode number concentration and solar zenith angle in the LMS. Nucleation mode number concentration (50th percentile, with interquartile range given by error bars) as a function of solar zenith angle at time of measurement in the LMS ($\text{O}_3 > 250 \text{ ppbv}$, $\text{RH} < 10 \%$) in the NH (a) and SH (b).

120

S3 Zonal mixing in the LMS

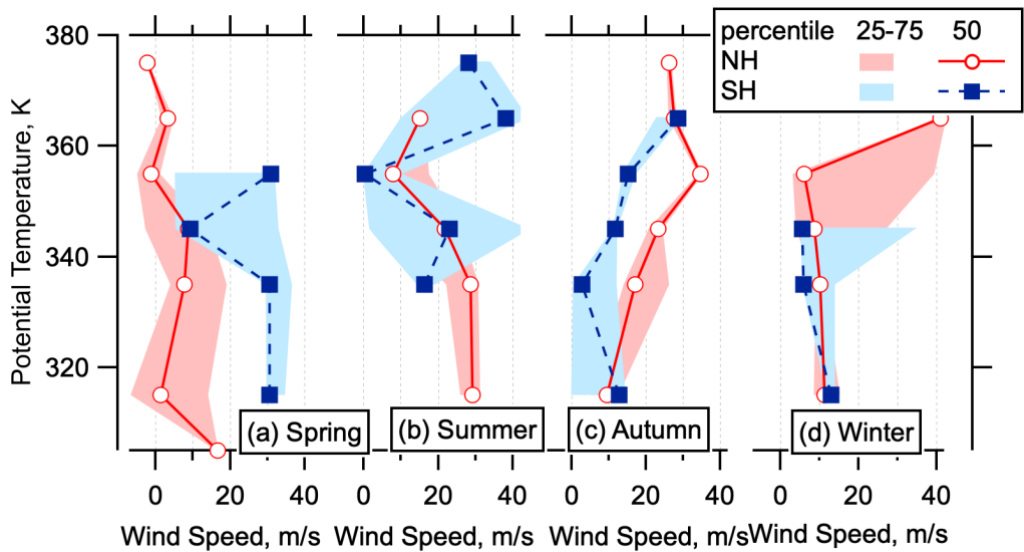


Figure S7: Horizontal windspeeds in the LMS. Horizontal windspeeds encountered on ATom in the LMS by season (a-d) and hemisphere (colours), as a function of potential temperature.

135

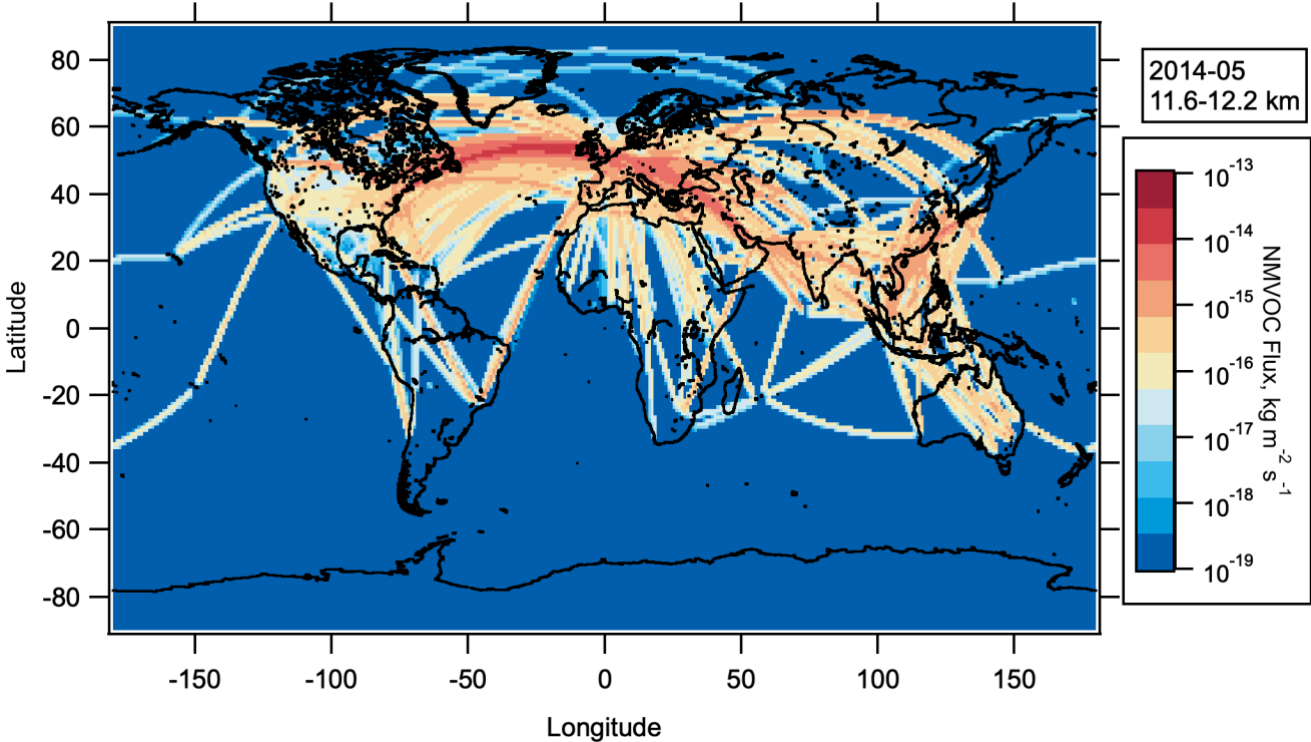


Figure S8: Spatial distribution of NMVOCs emitted by aircraft. NMVOC flux from aircraft from CEDS emissions database for May 2014, between 11.6 and 12.2 km altitude as a function of latitude and longitude. World map was made with Natural Earth Free Vector and Raster Map Data. <http://www.naturalearthdata.com> (accessed 10 December 2015).

140

145

150

S5. Volcanic Emissions

155 **Table S01: Volcanic activity relevant to ATom LMS observations.** Name, latitude, longitude and date of all volcanic eruptions within two months of ATom observations for the four deployments with observed peak emission heights above 7 km altitude. The altitude of the plume height of each eruption, and mass of SO₂ in each plume are given in km and kT respectively. Data are from the Multi-Satellite Volcanic Sulfur Dioxide (SO₂) Database Long-Term L4 Global.

* indicates that the plume altitude was was not measured by satellite and instead estimated as a fixed altitude above the vent (10 km for explosive eruptions, 5 km for effusive eruptions).

160 ** indicated that the altitude is estimated as for *, and that even though this estimate lies outside the altitude range we are considering, it is included here because of the larger uncertainty of the emission altitude

volcano	lat	lon	start date	end date	Altitude (km)	SO ₂ (kT)	SO ₂ NH (kT)	SO ₂ SH (kT)
Atom1 29.07.2016 - 23.08.2016						Total:	57	0
Etna	37.734	15.004	2016-05-18	2016-05-21	7	5		
Alaid	50.858	155.55	2016-07-04	2016-07-05	7.339*	2		
Kliuchevskoi	56.057	160.638	2016-07-06	2016-08-16	7.5	50		
ATom2 26.01.2017 - 21.02.2017						Total:	23.5	2
Chirinkotan	48.98	153.48	2016-11-28	2016-11-28	9	10		
Bogoslof	53.93	-168.03	2016-12-19	2017-01-27	7.6-10.7	10.5		
Fuego	14.473	-90.88	2017-01-26	2017-01-26	7	3		
Piton_de_la_Fournaise	-21.229	55.713	2017-02-01	2017-02-01	7.631*	2		
ATom3 28.09.2017 - 28.10.2017						Total:	0	80
Ambae	-15.4	167.83	2017-09-07	2017-09-07	6.496**	40		
Tinakula	-10.38	165.8	2017-10-20	2017-10-20	11	40		
ATom4 24.04.2018 - 21.05.2018						Total:	48	153
Fuego	14.473	-90.88	2018-02-01	2018-02-01	7	3		
Sinabung	3.17	98.392	2018-02-19	2018-02-19	17	15		
Kirishimayama	31.934	130.862	2018-03-06	2018-03-07	10	20		
Kirishimayama	31.934	130.862	2018-04-04	2018-04-04	10	10		
Ambae	-15.4	167.83	2018-04-05	2018-04-05	17	150		
Piton_de_la_Fournaise	-21.229	55.713	2018-04-28	2018-04-28	7.631*	3		

References

- Andreae, M. O., Afchine, A., Albrecht, R., Holanda, B. A., Artaxo, P., Barbosa, H. M. J., Borrmann, S., Cecchini, M. A.,
165 Costa, A., Dollner, M., Futterer, D., Jarvinen, E., Jurkat, T., Klimach, T., Konemann, T., Knote, C., Kramer, M., Krisna, T.,
Machado, L. A. T., Mertes, S., Minikin, A., Pohlker, C., Pohlker, M. L., Poschl, U., Rosenfeld, D., Sauer, D., Schlager, H.,
Schnaiter, M., Schneider, J., Schulz, C., Spanu, A., Sperling, V. B., Voigt, C., Walser, A., Wang, J., Weinzierl, B., Wendisch,
M., and Ziereis, H.: Aerosol characteristics and particle production in the upper troposphere over the Amazon Basin, *Atmos*
Chem Phys, 18, 921-961, 10.5194/acp-18-921-2018, 2018.
- 170 Bianchi, F., Trostl, J., Junninen, H., Frege, C., Henne, S., Hoyle, C. R., Molteni, U., Herrmann, E., Adamov, A., Bukowiecki,
N., Chen, X., Duplissy, J., Gysel, M., Hutterli, M., Kangasluoma, J., Kontkanen, J., Kurten, A., Manninen, H. E., Munch, S.,
Perakyla, O., Petaja, T., Rondo, L., Williamson, C., Weingartner, E., Curtius, J., Worsnop, D. R., Kulmala, M., Dommen, J.,
and Baltensperger, U.: New particle formation in the free troposphere: A question of chemistry and timing, *Science*, 352, 1109-
1112, 10.1126/science.aad5456, 2016.
- 175 Bianchi, F., Kurtén, T., Riva, M., Mohr, C., Rissanen, M. P., Roldin, P., Berndt, T., Crounse, J. D., Wennberg, P. O., Mentel,
T. F., Wildt, J., Junninen, H., Jokinen, T., Kulmala, M., Worsnop, D. R., Thornton, J. A., Donahue, N., Kjaergaard, H. G., and
Ehn, M.: Highly Oxygenated Organic Molecules (HOM) from Gas-Phase Autoxidation Involving Peroxy Radicals: A Key
Contributor to Atmospheric Aerosol, *Chem. Rev.*, 119, 3472-3509, 10.1021/acs.chemrev.8b00395, 2019.
- Höpfner, M., Boone, C. D., Funke, B., Glatthor, N., Grabowski, U., Günther, A., Kellmann, S., Kiefer, M., Linden, A., Lossow,
180 S., Pumphrey, H. C., Read, W. G., Roiger, A., Stiller, G., Schlager, H., von Clarmann, T., and Wissmüller, K.: Sulfur dioxide
(SO₂) from MIPAS in the upper troposphere and lower stratosphere 2002–2012, *Atmos. Chem. Phys.*, 15, 7017-
7037, 10.5194/acp-15-7017-2015, 2015.
- Murphy, D. M., Froyd, K. D., Bourgeois, I., Brock, C. A., Kupc, A., Peischl, J., Schill, G. P., Thompson, C. R., Williamson,
C. J., and Yu, P.: Radiative and chemical implications of the size and composition of aerosol particles in the existing or
185 modified global stratosphere, *Atmos. Chem. Phys. Discuss.*, 2020, 1-32, 10.5194/acp-2020-909, 2020.
- Nieminen, T., Lehtinen, K. E. J., and Kulmala, M.: Sub-10 nm particle growth by vapor condensation – effects of vapor
molecule size and particle thermal speed, *Atmos. Chem. Phys.*, 10, 9773-9779, 10.5194/acp-10-9773-2010, 2010.
- Orbe, C., Holzer, M., Polvani, L. M., Waugh, D. W., Li, F., Oman, L. D., and Newman, P. A.: Seasonal ventilation of the
stratosphere: Robust diagnostics from one-way flux distributions, *Journal of Geophysical Research: Atmospheres*, 119, 293-
190 306, <https://doi.org/10.1002/2013JD020213>, 2014.

- Schroder, F., Brock, C. A., Baumann, R., Petzold, A., Busen, R., Schulte, P., and Fiebig, M.: In situ studies on volatile jet exhaust particle emissions: Impact of fuel sulfur content and environmental conditions on nuclei mode aerosols, *J Geophys Res-Atmos*, 105, 19941-19954, Doi 10.1029/2000jd900112, 2000.
- Seinfeld, J. H., and Pandis, S. N.: *Atmospheric chemistry and physics from air pollution to climate change*, 2nd ed., Wiley, Hoboken, N.J., 1203 S. pp., 2006.
- Stolzenburg, D., Fischer, L., Vogel, A. L., Heinritzi, M., Schervish, M., Simon, M., Wagner, A. C., Dada, L., Ahonen, L. R., Amorim, A., Baccarini, A., Bauer, P. S., Baumgartner, B., Bergen, A., Bianchi, F., Breitenlechner, M., Brilke, S., Mazon, S. B., Chen, D. X., Dias, A., Draper, D. C., Duplissy, J., Haddad, I., Finkenzeller, H., Frege, C., Fuchs, C., Garmash, O., Gordon, H., He, X., Helm, J., Hofbauer, V., Hoyle, C. R., Kim, C., Kirkby, J., Kontkanen, J., Kuerten, A., Lampilahti, J., Lawler, M., Lehtipalo, K., Leiminger, M., Mai, H., Mathot, S., Mentler, B., Molteni, U., Nie, W., Nieminen, T., Nowak, J. B., Ojdanic, A., Onnela, A., Passananti, M., Petaja, T., Quelever, L. L. J., Rissanen, M. P., Sarnela, N., Schallhart, S., Tauber, C., Tome, A., Wagner, R., Wang, M., Weitz, L., Wimmer, D., Xiao, M., Yan, C., Ye, P., Zha, Q., Baltensperger, U., Curtius, J., Dommen, J., Flagan, R. C., Kulmala, M., Smith, J. N., Worsnop, D. R., Hansel, A., Donahue, N. M., and Winkler, P. M.: Rapid growth of organic aerosol nanoparticles over a wide tropospheric temperature range, *Proc. Natl. Acad. Sci. U.S.A.*, 115, 9122-9127, 10.1073/pnas.1807604115, 2018.
- Tröstl, J., Chuang, W. K., Gordon, H., Heinritzi, M., Yan, C., Molteni, U., Ahlm, L., Frege, C., Bianchi, F., Wagner, R., Simon, M., Lehtipalo, K., Williamson, C., Craven, J. S., Duplissy, J., Adamov, A., Almeida, J., Bernhammer, A.-K., Breitenlechner, M., Brilke, S., Dias, A., Ehrhart, S., Flagan, R. C., Franchin, A., Fuchs, C., Guida, R., Gysel, M., Hansel, A., Hoyle, C. R., Jokinen, T., Junninen, H., Kangasluoma, J., Keskinen, H., Kim, J., Krapf, M., Kürten, A., Laaksonen, A., Lawler, M., Leiminger, M., Mathot, S., Möhler, O., Nieminen, T., Onnela, A., Petäjä, T., Piel, F. M., Miettinen, P., Rissanen, M. P., Rondo, L., Sarnela, N., Schobesberger, S., Sengupta, K., Sipilä, M., Smith, J. N., Steiner, G., Tomè, A., Virtanen, A., Wagner, A. C., Weingartner, E., Wimmer, D., Winkler, P. M., Ye, P., Carslaw, K. S., Curtius, J., Dommen, J., Kirkby, J., Kulmala, M., Riipinen, I., Worsnop, D. R., Donahue, N. M., and Baltensperger, U.: The role of low-volatility organic compounds in initial particle growth in the atmosphere, *Nature*, 533, 527-531, 10.1038/nature18271, 2016.
- Yang, H., Chen, G., Tang, Q., and Hess, P.: Quantifying isentropic stratosphere-troposphere exchange of ozone, *Journal of Geophysical Research: Atmospheres*, 121, 3372-3387, 10.1002/2015jd024180, 2016.
- Zhu, J., Penner, J. E., Yu, F., Sillman, S., Andreae, M. O., and Coe, H.: Decrease in radiative forcing by organic aerosol nucleation, climate, and land use change, *Nat Commun*, 10, 423-423, 10.1038/s41467-019-08407-7, 2019.